EURASIAN PHYSICAL TECHNICAL JOURNAL

2025, Volume 22, No. 3 (53)

https://doi.org/10.31489/2025N3/75-83

Received: 18/04/2025 Revised: 05/06/2025 Accepted: 25/09/2025 Published online: 30/09/2025

Research Article

UDC 537.521:535.372

OPTICAL SPECTROSCOPIC DIAGNOSIS OF ELECTRON TEMPERATURE AND DENSITY FOR ZN-AL ALLOY PLASMA: EFFECT OF LASER ENERGY ON PLASMA PARAMETERS

Jawad, Mohammed H*, Abdulameer, M.R

University of Baghdad, College of Science, Department of Physics, Baghdad, Iraq
* Corresponding Author: mohammed.hamza1204a@sc.uobaghdad.edu.iq

Abstract: *In this study, the properties of plasma produced from zinc and aluminum alloy were investigated using laser spectroscopy techniques. The alloy was locally manufactured and consisted of 20 to 80 percent zinc and aluminum, respectively. Neodymium-doped Yttrium Aluminum Garnet (Nd:YAG) laser with a fundamental wavelength of 1064 nm was used with a variable laser energy from 500 to 900 mJ In order to study the behavior of plasma and determine its general properties such as electron density and temperature. Boltzmann plot method was employed to ascertain the temperature of the electrons, in addition to using Stark expansion method to calculate the electron density. Based on these two basic parameters, the rest of the additional plasma parameters were calculated and determined. The results obtained from this study showed that there is a clear effect of laser energy on the plasma parameters, as the temperature and electron density increased significantly with the increase in laser energy, as these parameters gradually increased with the increase of laser energy. The maximum value of the electron temperature was 0.918 eV at 900 MJ, while the electron temperature was 0.537 eV at 500 mJ. On the other hand, the results showed an increase in both the Debye number and plasma frequency at high laser energies, while the Debye length showed a clear decrease at high power. The main purpose of this study is to contribute to a deeper understanding of the properties of plasma and how laser power affects these properties, which opens the way for many applications, including engraving and marking on metals and many industrial and technological applications.*

Keywords: Zn-Al Alloy, Optical spectroscopy of plasma (OES), Plasma properties and parameters.

1. Introduction

The analytical technique known as laser-induced plasma spectroscopy is well-established. used to determine samples' elemental compositions at a very high speed. This method can be categorized as a form of atomic emission spectroscopy, which is typically employed to examine materials, regardless of whether they are solid, liquid, or gaseous [1]. There are many uses for Laser-Induced Breakdown Spectroscopy (LIBS), an emission spectroscopic method for characterizing the elements in materials. When the surface of a sample is ablated by a high-intensity laser pulse, a plasma plume is created. The ablated mass of the substance falls between nanograms and micrograms [2]. The irradiation settings have a direct impact on the rapidly developing properties of the laser-generated plasma., which are transient by nature. These factors include the laser's wavelength, the duration of its pulse, the intensity of the laser incident on the target's surface, and the ambient pressure [3].To summarize, a high-intensity laser pulse targets a tiny area of the sample surface to excite the optical sample, which is then evaluated [4]. Recent years have seen a great deal of research on optical emission from laser-generated plasmas, and the sample target's interaction with the

laser was utilized to determine the atomic and ionic line emission [5]. The study of the generated emissions will contribute greatly to the identification of the elements using the spectrometer. The process of diagnosing the plasma is done by calculating its main parameters such as its temperature and electron density. On the other hand, there is a clear effect of the target material and the parameters of the laser used [6, 7]. The Boltzmann plot equation which is stated as follows, is one of the best methods for determining The local thermodynamic equilibrium's electron temperature, In contrast, one of the most popular approaches for the Optical spectroscopy of plasma (OES) in this study is the ratio approach [8].

$$\ln\left[\frac{\lambda_{ji}I_{ji}}{hcA_{ji}g_j}\right] = \frac{1}{k_B T}(E_j) + \ln\left[\frac{N}{U(T)}\right] \quad (1)$$

Here, I_{ji} is the emission line intensity, λ_{ji} the wavelength, gj the statistical weight of the upper level, Aji the transition probability, E_j the excitation energy, k_B Boltzmann's constant, and Te the electron temperature. The Stark expansion method is used to determine the electron density using the equation below: [9].

$$n_e = \left(\frac{\Delta\lambda_{FWHM}}{2w}\right) N_r \quad (2)$$

Here, Δλ is the full width at half maximum (FWHM) of the spectral line, ne the electron density, and w the Stark broadening parameter. The line w, Nr≈10^{17} cm^{-3}, which theoretically represents the whole width of the Stark parameter, is represented by Full Width at Half Maximum (FWHM), which expresses the width at mid-intensity. The plasma frequency is adjusted so that electric fields are produced whenever its semi-neutral equilibrium is disturbed. Given that it solely depends on the plasma's density, this frequency is a very basic plasma factor. The plasma frequency can be computed using the formula below, which is inherently rather high due to the mince's small size [10]

One of the crucial factors is the Plasma frequency (fp) that are calculated in diagnostic processes, as the turbulent processes that occur lead to a disturbance of the quasi-equilibrium state in the plasma. The frequency is influenced by the density of plasma., can be calculated using the equation below [11].

$$f_p = \sqrt{\frac{e^2 n_e}{\varepsilon_0 m_e}} \quad (3)$$

Here, *fp* is the plasma frequency, *ne* the electron density, *e* the electron charge, *ε0* the permittivity of free space, and *me* the electron mass.

The main characteristic of plasma that is calculated is the Debye length (λD), which represents the distance at which the plasma is protected from the effects of the external electric field. The Debye length is inversely related to the electron density and is expressed mathematically using the equation below [12].

$$\lambda_D = \sqrt{\left(\frac{\epsilon_0 k_B T_e}{n_e e^2}\right)} = 7430 * \sqrt{\frac{T_e}{n_e}} \quad (4)$$

Here, *λD* is the Debye length, *Te* the electron temperature, *ε0* the permittivity of free space, *kB* Boltzmann's constant, *ne* the electron density, and *e* the electron charge.

Comparing the system dimension to this basic prerequisite for plasma existence (λD < < < L), the Debye length should be relatively tiny. The second need for plasma existence (Debye number (ND)>>>1), which depends as follows on the electron temperature and density [13-15]

$$N_D = \frac{4}{3}\pi n_e \lambda_D^3 \quad (5)$$

Here, *ND* is the Debye number, *ne* the electron density, *λD* the Debye length, and *V* the plasma volume. The primary goal of this research is to investigate the effect of laser beam energy on the behavior of induced plasma produced from zinc and aluminum alloys in order to provide a deeper and more comprehensive understanding of how laser energy interacts with different materials, which could open up great horizons in many industrial and technological applications, especially those applications that include this type of process.

2. Experimental section

2.1 Preparing Zinc-aluminum alloy

A locally produced zinc-aluminum alloy with a purity of (99.99%) was prepared using a gas smelting method. This alloy consists of 80% zinc and 20% aluminum. The zinc was melted at a temperature of 550°C, after which aluminum was added in lumps, and the mixture was mixed using a diffusion method. The gas smelting method offers many advantages, as it provides better control over the temperature of the elements,

which helps in pouring the alloy evenly and accurately. In addition, it is cost-effective compared to other methods, and it provides a cleaner environment and is less polluted than traditional fuels. A square sample of the alloy, measuring (2 x 2 cm) and 3 mm thick, was positioned 10 cm away from the laser lens after that to get it ready for the procedure of ablation. Figure 1 shows the alloy used in the study.

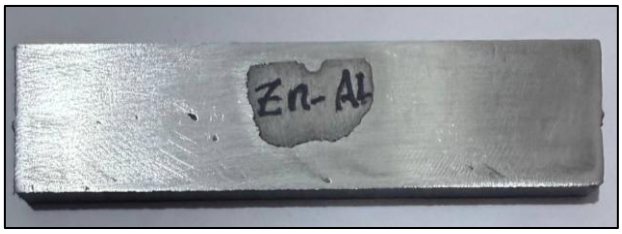

Fig 1: Cross section of zinc aluminum alloy

2.2 Configuring the laser-induced spectroscopy system

In this study, plasma was generated by a pulsed Nd:YAG laser operating at 6 Hz and a wavelength of 1064 nm. A target surface, placed 10 cm away, was illuminated by the beam at a 45° angle. This beam ionized and vaporized the material, creating plasma above the surface. This experiment was conducted at atmospheric pressure with pulse rates ranging from 15 to 30 pulses. Wavelength spectra were then obtained by placing a Sarwat (S3000)-UV-NIR spectrometer 1 cm from the target surface of the sample, as shown in Figure 2. These spectra were recorded for all laser energies used, ranging from 500 to 900 mJ, and compared with the National Institute of Standards and Technology (NIST) data shown in Table 1. This technique was used to determine the plasma parameters of the alloys used.

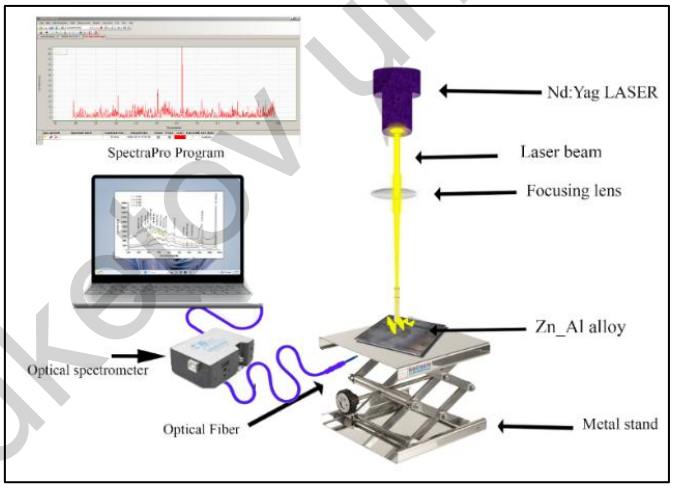

Fig 2: Basic components of an induced laser spectroscopy system

Table 1: Basic parameters of Zn-Al Alloy plasma

Element	Intensity	λ (nm)	g_kA_{ki} (S^{-1})	E_K (eV)
AL I	397.63	226.3462	8.80E+07	5.568835
	628.51	236.7052	5.58E+08	3.816692
	6530.41	308.2151	4.50E+08	6.192025
	7586.39	394.40058	8.72E+07	7.737027

3. Results and Discussion

The spectra in Figure 3 clearly show the increase in emission line intensities with increasing laser energy. The most pronounced variations were observed at the Al I line (394.40 nm) and the Zn I line (636.23 nm), which exhibit systematic intensity enhancement as the laser fluence increases. These lines were therefore selected as representative indicators of the effect of laser energy on plasma emission.

The above data shows that the emission lines of the spectrum increase with increasing laser power. The main reason for this is that as the power increases, the ablation of the metal (target) increases, resulting in increased plasma emission. More than one emission line was recorded for the alloying elements. The highest peak for aluminum was at a wavelength of 394.400 nm, while the highest peak for zinc was at a wavelength of 636.23 nm. Emissions from nitrogen and oxygen gases were also recorded. The nitrogen peak reached 480.0 nm, while the oxygen peak was recorded at 435.45 nm [16].

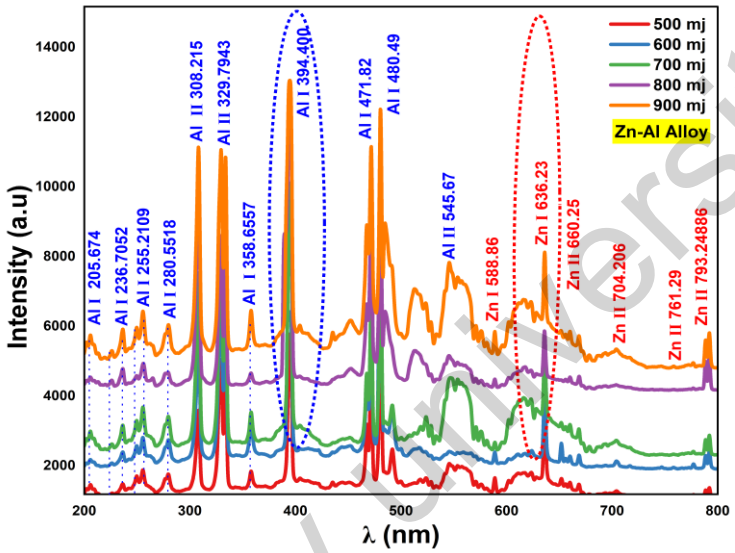

Fig.3. Laser-Induced Plasma Emission Spectra on an Al-Zn Alloy Target at Various Laser Energies

The variation of spectral line intensities with laser energy does not follow a strictly linear trend. This non-linearity can be explained by self-absorption of emitted radiation at higher plasma densities, plasma shielding effects that reduce the effective laser energy reaching the target, and enhanced collisional processes (electron–ion and electron–neutral) which modify the population of excited states. These combined mechanisms result in deviations from linear behavior for some spectral lines.

According to Equation 1, the Electron temperature (Te) in the zinc-aluminum alloy plasma in this study was determined using the Boltzmann diagram method. Considering the existence of thermodynamic equilibrium, the slope of the curve drawn between $Ln(\lambda jiIji/gjAji)$ and energy is the criterion for applying the Boltzmann diagram method. Four atomic lines of aluminum (Al I) were used, all in the same atomic transition state. The temperature was calculated by taking the reciprocal of the slope ($-1/kBT$). The R2 criterion is an indicator of the degree of agreement of the result, also known as the statistical coefficient, and its value always ranges from 0 to 1, with the best result being close to 1. Figure 4 shows the Boltzmann correlation diagram.

The findings indicated that the temperature of electrons is directly related to the laser beam energy, with a gradual increase observed at all laser energies used. This is because as the laser energy increases, more energy is transferred to the electrons [17]. The higher the energy, the greater the amount of energy transferred, and consequently, the mobility of these electrons increases, leading to an increase in their temperature. The temperature at an energy of 500 millijoules was found to be 0.537 electron volts, while at a temperature of 900 millijoules, it was 0.918 electron volts. The electron temperature (Te) shows an almost linear increase with laser energy.

This behavior can be explained by the direct coupling of the laser pulse with the plasma electrons. As the laser fluence increases, a larger number of free electrons are generated and these absorb the incident radiation mainly through inverse Bremsstrahlung and collisional excitation, converting the laser energy into electron thermal energy.

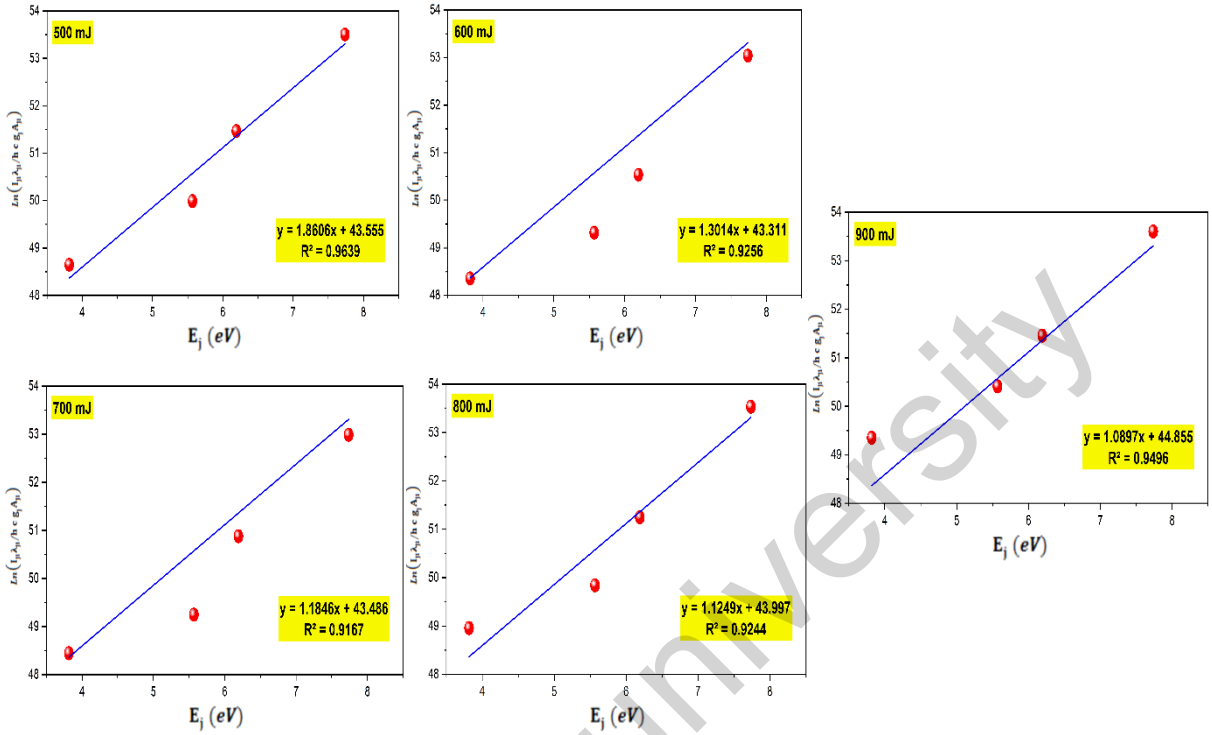

Fig 4. Zn-Al alloy plasma's Boltzmann plot was determined using a range of laser intensities.

Under the present experimental conditions, the rate of this energy transfer is approximately proportional to the laser energy, which results in the observed near-linear dependence. The figure 5 shows the electron temperature of a zinc-aluminum alloy in electron volts and kelvins.

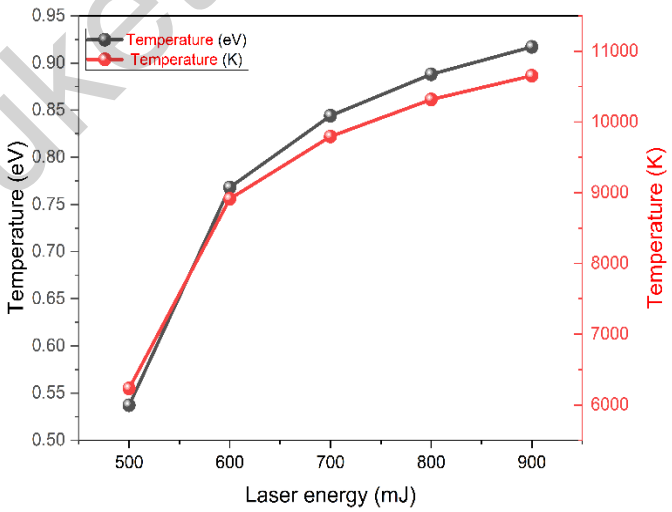

Fig 5. Electron temperature of zn-al alloy in electron volts and kelvin at varying laser intensities (500-900 mJ).

The Stark broadening method was used to calculate the Electron density (ne). This method is based on measuring he amplitude of the spectral lines and calculating the width at the midpoint of the intensity. The laser-induced emission spectrum of zinc and aluminum alloys exhibits broad lines, as shown in Figure 6.

These lines are primarily affected by their high amplitude. This is caused by collisions between charged particles and the emitting atoms. Equation (2) was used to calculate the electron density based on the spectral line width. The AL spectral emission line at 394.400 nm was used to calculate the electron density for the various energies used. The results obtained showed that the electron density is directly affected by the laser beam energy, showing a clear increase at higher energies. The maximum electron density at a laser energy of 500 mJ was $5.4*10^{17}$ (cm^{-3}), while the highest density at a laser energy of 900 mJ was $9.61*10^{17}$ (cm^{-3}). This demonstrates that when laser intensity increases, the electron density rises noticeably.

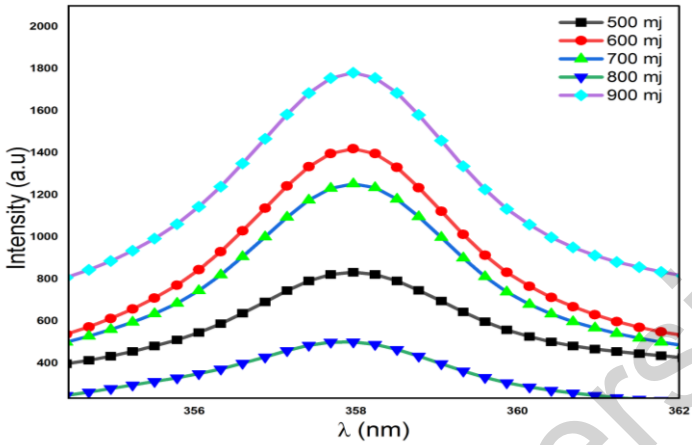

Fig.6. The Zn-Al alloy spectrum's full width at half maximum (FWHM) at 356-364 nm at various laser energy levels (Lorentzian Fitting).

To more accurately describe the properties of the zinc-aluminum plasma, Laser beam energy's impact on other plasma properties were examined. It was found that increasing the energy directly and significantly affects these other fundamental parameters, such as the (λD), (fp), and (N_D). Equations 3, 4, and 5 were used to obtain the data shown in Table 2, which indicate that the plasma frequency fp and N_D will increase significantly When the laser's energy increases. This is due to the fact that frequency and density are directly correlated, and the number of collisions increases at higher energies due to the increased amount of energy transferred from the laser beam to the resulting plasma. The peak plasma frequency was recorded at an energy of 500 mJ, while the peak frequency was recorded at an energy of 900 mJ. These findings also revealed a noteworthy increase in Nd with increasing laser beam energy. This is because that higher laser energy leads to increased interaction with the sample, resulting in the formation of more particles as a result of this interaction. On the other hand, increasing laser energy leads to a decrease in λD. This is because higher laser energy causes increased movement of plasma particles due to the greater energy they gain. This movement will cause the distance between the particles to decrease. The greater the energy, the more interactions between the particles increase, and the closer they become. In other words, the Debye length depends on the temperature of the electrons. Since increasing laser energy leads to an increase in the temperature of the electrons, this will in turn lead to a decrease in the Debye length [18].

Table 2: Features of the Zn-Al alloy plasma produced at various laser energies using a 1064 nm laser

E (mJ)	Te (eV)	n_e *10 ^{17} (cm^{-3})	f_p * 10^{+12} (Hz)	λ_D*10^{-6} (cm)	N_d *10^3
500	0.537	5.49	6.7	2.0	0.913
600	0.768	6.74	7.4	1.8	1.409
700	0.844	8.62	8.3	1.6	1.435
800	0.889	9.51	8.8	1.4	1.476
900	0.918	9.61	8.9	1.3	1.540

Figure 7 illustrates how laser power significantly affects the electron temperature and density. We observe that the Te gradually increases from 0.537 to 0.918 eV with increasing laser intensity. The results also show that the electron density increases from 5.49 to 9.61 with increasing laser power. The main reason

for this increase is the increase in laser pulse energy, which significantly affects the emission lines' intensity. This, in turn, affects the increase in these parameters.

Figure 8 shows the frequency of plasma rises and the Debye length decreases with increasing laser intensity. The frequency values range from 6.7 * 10^{12} to 8.9 * 10^{12} Hz, and 500-900 mJ is the laser power range. Equation 3 states that since the frequency and density are directly related, the frequency increase is natural. Equation 4 asserts that the relationship between the Debye length and the electron density is inverse. and decreases as the laser power increases. Its values are between 1.5 * 10^{-6} cm-3 and 2 * 10^{-6}. These results are consistent with the results of Maryam and Khadem (2021) [1].

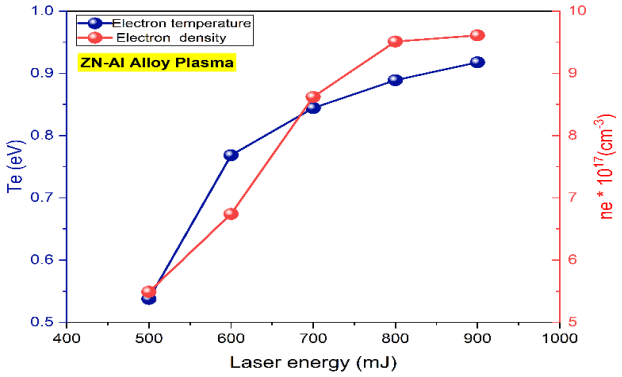

Fig.7. Zn-Al alloy's Te and Ne differences as a function of laser power at various energy levels

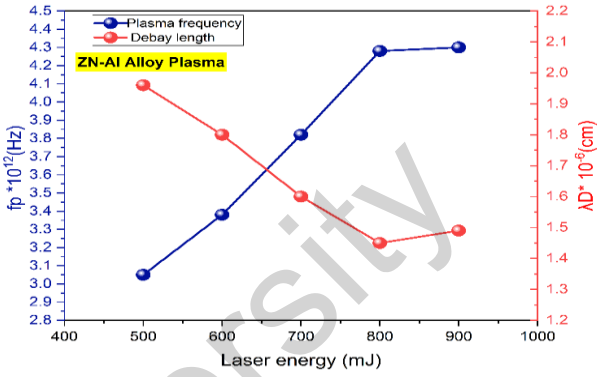

Fig.8. Zn-Al alloy's fp and λD differences with laser power at various energy levels

Figure 9 shows the clear increase in the number of particles in the Debye sphere in relation to laser intensity. This can be explained by the fact that increasing the laser power will have a significant effect on the particles that make up the plasma, making them move at a faster speed, which increases their interactions in the medium.

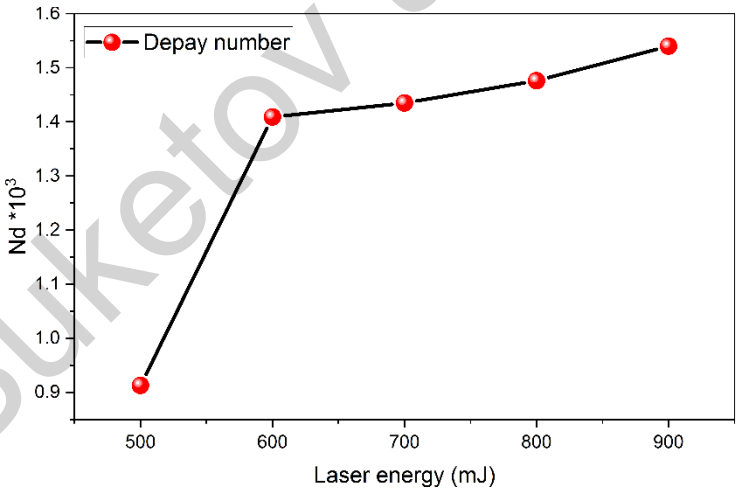

Fig. 9. Zn-Al alloy plasma's Debye number at varying laser energies

That is, the distances that the particles penetrate will be larger, meaning that the number of ionized atoms will become greater, and thus additional quantities of charged particles (electrons or ions) will be released. these results are consistent with [19].

4. Conclusion

This study focused on optical spectroscopy (OES) to characterize the plasma properties generated using a 1064 nm Nd:YAG laser from locally manufactured zinc-aluminum alloys with fabrication percentages ranging from 20% to 80%. The primary objective was to determine the basic plasma parameters, such as electron density and electron temperature, and to study the effect of laser beam energy on these properties

and the emissions associated with plasma formation. The Boltzmann diagram and Stark expansion were used to calculate both the electron density and temperature. The results showed that the highest value was obtained at 900 mJ, with the electron temperature reaching 0.918 eV, compared to 0.537 eV at 500 mJ. The results also showed that increasing laser power significantly affects secondary plasma properties, such as the Debye length, plasma frequency, and Debye number. Both the plasma frequency and Debye number increase with increasing energy, while the Debye length decreases with increasing energy. Thus, it is clear that the laser power plays a crucial role in controlling the plasma properties and parameters in locally manufactured Zn–Al alloys.

Conflict of interest statement

The authors declare that they have no conflict of interest in relation to this research, whether financial, personal, authorship or otherwise, that could affect the research and its results presented in this paper.

Credit author statement

Jawad, Mohammed H.: Conceptualization, Methodology, Writing - original draft**; Abdulameer, Mohammed R.:** Data Curation**,** Investigation; Review & Editing, Validation.

The final manuscript was read and approved by all authors.

References

1. Abbas Z.M., Abbas Q.A. (2024) Aluminum-doped ZnO nano-laminar structures by pulsed laser ablation for gas sensing application. *Journal of Optics, 53*(2), 544–557. https://doi.org/10.1007/s12596-023-01192-z
2. Aadim K.A. (2019) Spectroscopic studying of plasma parameters for SnO_2 doped ZnO prepared by pulse Nd:YAG laser deposition. *Iraqi Journal of Physics, 17*(42), 125–135. https://doi.org/10.30723/ijp.v17i42.447
3. Ahmed R.T., Ahmed A.F. (2024) Optical emission spectroscopy characteristics of chromium plasma parameters. *Journal of Optics, 53*(2), 1590–1597. https://doi.org/10.1007/s12596-023-01336-1
4. Ahmed R.T., Ahmed A. F., Aadim K.A. (2024) Influence of laser energy on structural and morphology properties of CdO and CdO: Sn production by -induced plasma. *Journal of Optics, 53*(2), 1564–1573. https://doi.org/10.1007/s12596-023-01291-x
5. Alkareem R.A., Ahmed B.M. (2025) Influence of laser energy on optical emission spectroscopy characteristics for zinc plasma parameters. *Journal of Optics, 29,* 1–6.https://doi.org/10.1007/s12596-025-02472-6
6. AlRashid S.N., Majeed N.F., Azeez M.A., Mazhir S.N. (2025) Calculating plasma parameters for Zn target using laser-induced breakdown spectroscopy. *Journal of Optics, 28,* 1–7. https://doi.org/10.1007/s12596-025-02644-4
7. Chen F.F. (2015) *Introduction to plasma physics.* Springer Science & Business Media. https://doi.org/10.1007/978-3-319-22309-4
8. Fahem M.Q., Jawad M.H., Abdulsada R.O., et al. (2025) The structure and electrical properties of $NiFe_2O_4$ and $NiMgFe_2O_4$ prepared via sol–gel method. *Ionics, 31,* 6475–6481. https://doi.org/10.1007/s11581-025-06333-x
9. Iftikhar A., Jamil Y., Nazeer N., Tahir M.S., Amin N. (2021) Optical emission spectroscopy of nickel-substituted cobalt–zinc ferrite. *Journal of Superconductivity and Novel Magnetism, 34,* 1849–1854. https://doi.org/10.1007/s10948-020-05734-5
10. Jamali S., Khoso M. A., Zaman M. H., Jamil Y., Bhutto W.A., Abbas A., Mari R.H., Kalhoro M.S., Shaikh N.M. (2021) Elemental analysis of kohl using laser ablation and atomic absorption spectroscopy (AAS) techniques. *Physica B: Condensed Matter, 620,* 413278. https://doi.org/10.1016/j.physb.2021.413278
11. Jawad M.H., Abdulameer M.R. (2023) The effect of background argon gas pressure on parameters of plasma produced by DC glow discharge. *Iraqi Journal of Science, 64*(3), 1210–1218. https://doi.org/10.24996/ijs.2023.64.3.17
12. Jawad M.H., Abdulameer M.R. (2024) Study the effect of external voltage on some plasma parameters produced by DC glow xenon gas discharge. *AIP Conference Proceedings, 2922*(1), 150003. https://doi.org/10.1063/5.0183126
13. Jawad M.H., Abdulameer M.R. (2025) Spectral analysis of brass plasma generated by a Nd:YAQ laser at λ = 1064 nm. *Russian Physics Journal, 68,* 903-911. https://doi.org/10.1007/s11182-025-03509-w
14. Jawad M.H., Abdulameer M.R. (2025) Spectroscopic investigation of plasma from Al–Ni alloy using OES technique: Influence of voltage on plasma parameters. *Indian Journal of Physics,* https://doi.org/10.1007/s12648-025-03738-2
15. Jawad M.H., Abdulameer M.R., Aadim K.A. (2025) Spectral diagnostics of Al–Ni alloys under laser irradiation: Effect of laser energy on plasma parameters. *Scientific and Technical Journal of Information Technologies, Mechanics and Optics, 25*(4), 626–634. https://doi.org/10.17586/2226-1494-2025-25-4-626-634
16. Kadhem S.J. (2023) Preparation of Al_2O_3/PVA nanocomposite thin films by a plasma jet method. *Science and Technology Indonesia, 8*(3), 471–478. https://doi.org/10.26554/sti.2023.8.3.471-478

17. Khaleel S.F., Aadim K.A. (2025) Investigation study of the plasma parameters for bronze produced by Nd:YAG laser at wavelength 1064 nm: Effect of laser energies. *Journal of Optics,* 1–6. https://doi.org/10.1007/s12596-025-02698-4

18. Mansour S.A.M. (2015) Self-absorption effects on electron temperature-measurements utilizing laser induced breakdown spectroscopy (LIBS) techniques. *Optics & Photonics Journal, 5*(3), 79–90. https://doi.org/10.4236/opj.2015.53007

19. Mohammed R.S., Aadim K.A., Ahmed K.A. (2022) Spectroscopy diagnostic of laser intensity effect on Zn plasma parameters generated by Nd:YAG laser. *Iraqi Journal of Science, 63*(9), 3711–3718. https://doi.org/10.24996/ijs.2022.63.9.5

20. Murtaza G., Shaikh N.M., Kandhro G.A., Ashraf M. (2019) Laser induced breakdown optical emission spectroscopic study of silicon plasma. *Spectrochimica Acta Part A: Molecular and Biomolecular Spectroscopy, 223,* 117374. https://doi.org/10.1016/j.saa.2019.117374

21. Oyebola O.O. (2017) Long wave-infrared laser-induced breakdown spectroscopy emissions from potassium chloride (KCl) and sodium chloride (NaCl) tablets. *Journal of Scientific Research & Development, 17,* 54–56. https://doi.org/10.4302/plp.2011.4.15

22. Rashid T.M., Rahmah M.I., Mahmood W.K., Fahem M.Q., Jabir M.S., Bidan A.K., Adbalrazaq S., Jawad M.H., Awaid D.M., Qamandar M.A., Alsaffar S.M. (2025) Eco-friendly laser ablation for synthesis of CNF@ Au nanoparticles: Insights into enhancing NO_2 gas detection and antibacterial activity. *Plasmonics.* https://doi.org/10.1007/s11468-025-02874-z

23. Shehab M.M., Aadim K.A. (2021) Spectroscopic diagnosis of the CdO: CoO plasma produced by Nd:YAG laser. *Iraqi Journal of Science, 62*(9), 2948–2955. https://doi.org/10.24996/ijs.2021.62.9.11

24. Turki Z.T., Fahem M.Q., Mankhi Z.A., et al. (2025) Magnetic field effect on cadmium oxide plasma properties detected by laser spectroscopy. *Russian Physics Journal,* 68, 804-812. https://doi.org/10.1007/s11182-025-03497-x

25. Wang J., Li X., Wang C., Zhang L., Li X. (2018) Effect of laser wavelength and energy on the detecting of trace elements in steel alloy. *Optik, 166,* 199–206. https://doi.org/10.1016/j.ijleo.2018.04.018

AUTHORS' INFORMATION

Jawad, Mohammed H. – PhD, Professor, Department of Physics, University of Baghdad, Baghdad, Iraq; SCOPUS Author ID: 56971327800; https://orcid.org/0000-0002-7395-9840; mohammed_plasma@sc.uobaghdad.edu.iq

Abdulameer, Mohammed R. – PhD Student, Department of Physics, University of Baghdad, Baghdad, Iraq; SCOPUS Author ID: 58536603200; https://orcid.org/0009-0001-8111-8195; mohammed.hamza1204a@sc.uobaghdad.edu.iq